

# Modelling and processing of interference pattern images produced by the Linnik interferometer

O. Kravchenko

National Technical University «Kharkiv Polytechnic Institute», Kyrpychova str., 2, 61002, Kharkiv, Ukraine.  
[Oleksandr.Kravchenko@cs.khpi.edu](mailto:Oleksandr.Kravchenko@cs.khpi.edu)

## Abstract

The paper is dedicated to the reconstruction of the relief profile of a mirror surface based on its interference pattern image. A mathematical model of the interferometer is constructed, which allows synthesising images of the interference pattern according to the given surface relief and microinterferometer settings. The model account for non-idealities of the optical path of the microinterferometer and the receiver. An algorithm based on interference fringe tracking is developed, which allows determining the height of each point of the image relative to some zero level, i.e. determination of the surface relief. The constructed models and algorithms are implemented in the form of a software package that allows both modelling the image of interference patterns and reconstructing the surface relief from real images obtained with the help of the interferometer. Testing of the software was carried out by using a numerical experiment, in the course of which the relief parameters similar to real ones were used. The constructed models, methods, and software can be used both in scientific research and in industrial laboratories, as well as for creating training samples and training of machine vision systems.

**Keywords:** interferometry, interference pattern, synthetic image, computer vision, surface topography reconstruction.

Received: 19.04.2025

Edited: 25.04.2025

Approved for publication: 30.04.2025

## Introduction

A new field of physics – physics of the surface of solid bodies – has recently been undergoing rapid development. Particular attention is drawn to the processes occurring on the surface following the radiation exposure, as a result of which the surface undergoes changes. The magnitude and types of these changes can provide information about the processes that produced these changes.

There are many techniques for studying the surfaces of solids, which are to be applied depending on the given task. Interference microscopy is an effective analytical tool for the non-contact study of surface morphology. In recent years, interferometry techniques have rapidly

been developed in terms of control of microrelief, deformation, and cleanliness of metal surfaces [1]. It is possible to estimate the size of damage due to the high sensitivity and accuracy of interference devices.

The feature of interferometry application in radiation physics of the surface lies in the fact that on experiencing radiation exposure, a stepped relief of the surface is often formed. This in turn makes interference fringes discontinuous, which complicates automatic processing of interferograms. In addition, the presence of steps produces a contrast microimage, which is clearly visible against the background of the interference pattern. Figure 1 gives examples of such features. Fig. 1a corresponds to an optically smooth surface of an

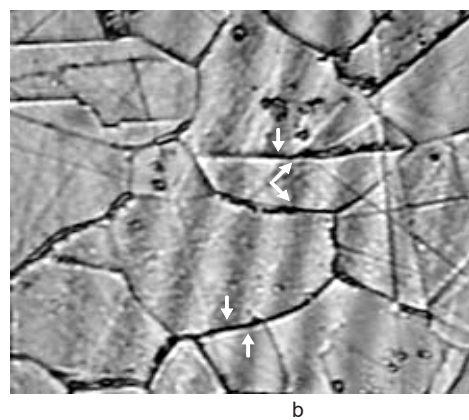
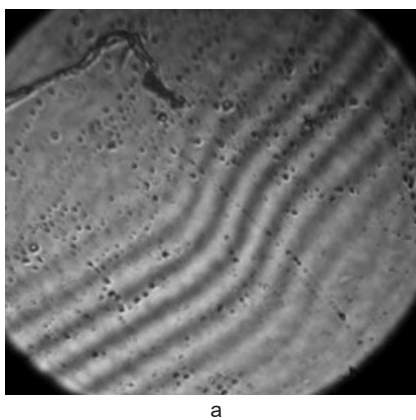


Fig. 1 Photographs of the surfaces: (a) with a smooth step on the amorphous material sample; (b) with interference fringe discontinuity on the stainless steel sample

amorphous metal with a smooth step, on which the presence of relief is visible only by distortion of interference fringes [1]. On the other hand, Fig. 1b shows a fragment of a stainless steel surface after ion bombardment, on which the contrasting relief and fringe discontinuities (shown by arrows in the figure) at grain boundaries are clearly visible [1].

**Problem statement**

The purpose of the study is to develop mathematical software and software for the automated surface relief reconstruction using computer processing of interference pattern photographs. Unlike the known analogues [2-4], the mathematical software accounts for the characteristic features of the surface exposed to radiation.

**Modelling of the interference pattern (direct problem)**

Wave interference is a phenomenon of amplification or weakening of the amplitude of the resulting wave depending on the ratio between the phases of two (or several) coherent waves folded in space [5].

Fig.2 shows the scheme of the micro-interferometric setup based on the Linnik MII-4 interferometer [6]. The beam  $L$  from the light source is split by intensity into two beams  $L_1$  and  $L_2$ .  $L_1$  is reflected from the reference mirror and once again from the beam splitter, and falls on the plane  $S$ . The  $L_2$  beam is reflected from the sample surface and also falls on the  $S$  plane. The interference pattern is formed as a result of the addition of  $L_1$  and  $L_2$  in the  $S$  plane. The path difference  $\Delta$ , equal to the difference of optical lengths travelled by these two beams, is determined by the presence of relief features in the sample, which leads to a phase difference of the interfered beams  $\delta=2p\Delta/\lambda$  ( $\lambda$  is the wavelength of light) [5]. The interference pattern formed on the plane  $S$  is recorded by a CCD matrix and transmitted to a computer via a USB interface.

When the intensities  $I'$  of the folded oscillations are equal, the distribution of the total light intensity  $I$  in the interference pattern is determined by the wavelength of the source radiation  $\lambda$ , the intensity of the two coherent folded beams  $I'$ , and the path difference  $\Delta$  between them:

$$I = 4I'(1 + \cos \delta) = 4I' \cos^2 \frac{\delta}{2} = 4I' \cos^2 \frac{\pi\Delta}{\lambda}. \quad (1)$$

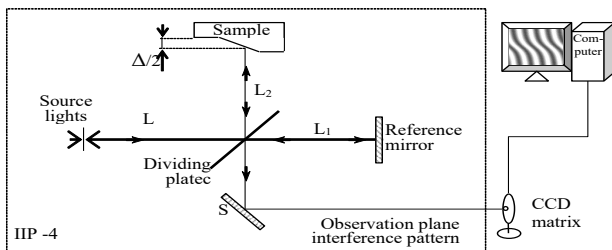


Fig. 2 Schematic diagram of the setup based on the Linnik microinterferometer MII-4 and computer

The MII-4 optics are structurally designed so that, regardless of the sample, the  $L_1$  beam front has a phase gradient. As a result, in the case of a perfectly smooth and flat sample surface, the interference pattern is a

sequence of parallel alternating dark and light stripes, the distance, width and direction of which are determined by the device parameters and can be varied.

If there are any deviations from flatness on the sample surface, the course of the fringes is distorted. Figure 3 shows the interference pattern corresponding to a sample whose surface is a smooth step. The parameters of the interference pattern are:  $b$  is the distance between the centres  $T$  of the neighbouring fringes coinciding with the extreme value of intensity (*min* is for dark and *max* is for light fringes);  $a_i$  is the fringe displacement, which is the distance between extremes  $T$  and  $T_i$ .

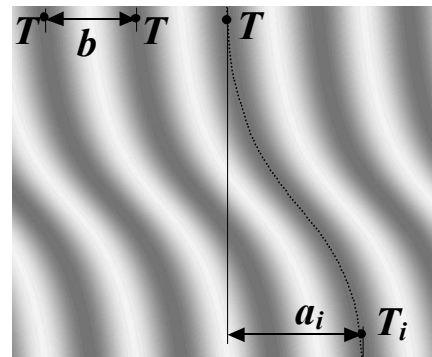


Fig. 3 Interference pattern corresponding to a surface with a smooth step:  $a_i$  — fringe shift on roughness,  $b$  — fringe width

A smooth step in the interference pattern leads to bending of the interference fringes, by the value of which one can determine the height of the step and assess the rate of change in height: the steeper the height difference on the surface, the sharper the fringes are shifted to the side.

To understand the influence of different relief forms on the appearance of the interference pattern and to certify the algorithms of their processing, it is necessary to be able to model the interference pattern according to the given relief and device features. The model should take into account, if possible, all factors affecting the formation of the real interference pattern.

Modelling consists of obtaining an interference pattern from the available surface topography. When modelling an ideal interference pattern, the shape of the surface is given by the function  $S(x,y)$ , and the intensity  $I(x,y)$  is calculated according to the following expression from formula (1):

$$I(x,y) = 4I'_{const} \cos^2 \left( \frac{\pi(\Delta_{const} + S(x,y))}{\lambda} \right), \quad (2)$$

where  $4I'_{const}$  is the maximum intensity value of the modelled interference pattern.

Figure 4 shows a cross section of the intensity distribution in the real interference pattern (shaded area) and the ideal data with the same period (solid line).

The intensity distribution over the field of a real interference pattern is not smooth and uniform. As can be seen from the inset to Fig. 4, this leads to displacement of extrema (shown by arrows) and, consequently, to distortion of information about the relief structure.

The intensity distribution is a hardware function of the instrument and changes only when the instrument

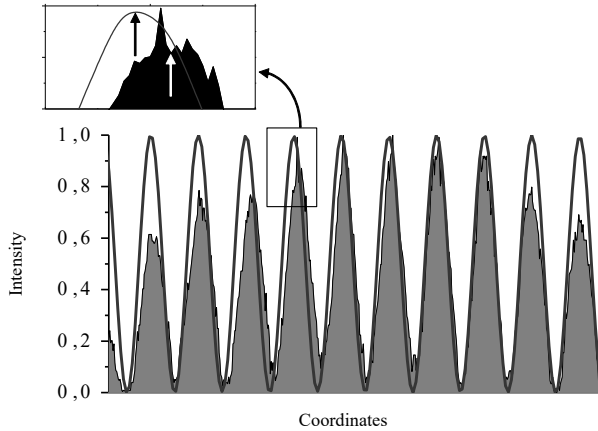


Fig. 4 Cross section of the intensity distribution over the field of the interference pattern. Inset: displacement of extrema in enlarged scale

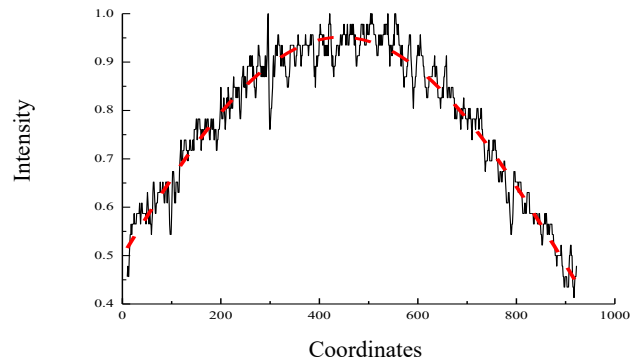


Fig. 5 Instrument illuminance intensity distribution (solid curve) and approximation by the Cauchy distribution (dashed line)

is readjusted. Thus, the influence of this function on the resulting intensity distribution can be taken into account in the model of the interference pattern and compensated when processing the interferogram. To this end, it is necessary to build a model of the function determining the inhomogeneity of illumination and additively include it in expression (2).

Fig. 5 shows the illumination cross section of the instrument's field of view and its mathematical model in the form of the Cauchy distribution [7].

The two-dimensional Cauchy distribution has the following form [7]:

$$\Phi(x, y) = f(x) \cdot f(y) = \frac{\theta^2}{\pi^2} \cdot \frac{1}{(\theta^2 + [x - \eta]^2)} \cdot \frac{1}{(\theta^2 + [y - \eta]^2)}, \quad \theta > 0, \quad (3)$$

where  $h$  is the median of the distribution,  $q$  is the scale parameter.

In addition, random factors related to the white noise of the CCD, source, etc. are superimposed on the interference pattern. This is also an additive interference, which can be modelled by a two-dimensional random Gaussian field.

Thus, the mathematical model of the interference pattern, taking into account all the above factors, has the following form:

$$I(x, y) = 4I'_{const} \cos^2 \left( \frac{\pi (\Delta_{const} + S(x, y))}{\lambda} \right) + \Phi(x, y) + n(x, y), \quad (4)$$

where the first summand is the contribution from the ideal picture,  $\Phi(x, y)$  is the illumination inhomogeneity function,  $n(x, y)$  is white noise.

Thus, in order to extract a clean signal and more accurately determine the position of the fringe extremum, one shall be able to construct a filter to compensate for noise and inhomogeneity when processing real interference patterns.

The constructed mathematical model and the algorithm developed according to it allow to carry out

modelling of the interference pattern according to the given parameters of the micro-interferometer, wavelength and function defining the surface, as well as such characteristics as the noise amplitude of the recording CCD matrix and inhomogeneity of the light field.

#### Surface profile reconstruction (inverse task)

The inverse task is to reconstruct the surface microrelief from its interference pattern. In this case, the accuracy of interference pattern processing and surface reconstruction is greatly influenced by the quality of the image itself.

The development of image recognition methods is a non-trivial task and requires an individual approach in each case.

The task of this work is to develop mathematical and software for automated restoration of surface relief using computer processing of interference pattern photographs. For the first time the approach to the algorithm creation is described, the main feature of which is adaptation to different types of interference patterns and adjustment of the algorithm to each without the experimenter's intervention.

As a result, a special software package (PC) "Linnik" has been created, which uses original mathematical and algorithmic software based on the idea of fringe tracking to reconstruct the relief from the interferogram. The main problem in solving such problems is the presence of a significant level of intensity distortion of different parts of the interference pattern. They are related both to the hardware (source fluctuations, defects in the optical path and white noise of CCD matrices) and to the characteristics of the investigated surface (roughness, inhomogeneity, etc.). The created algorithms are highly resistant to such distortions due to the use of special mathematical methods.

The block diagram of the surface reconstruction algorithm created in this work is shown in Fig.6. The scheme consists of three main actions: preparation of initial data (step 0), determination of the mean lines of all interference fringes (steps 1 and 2) and calculation of the surface relief (step 3). Let us consider each of the stages.

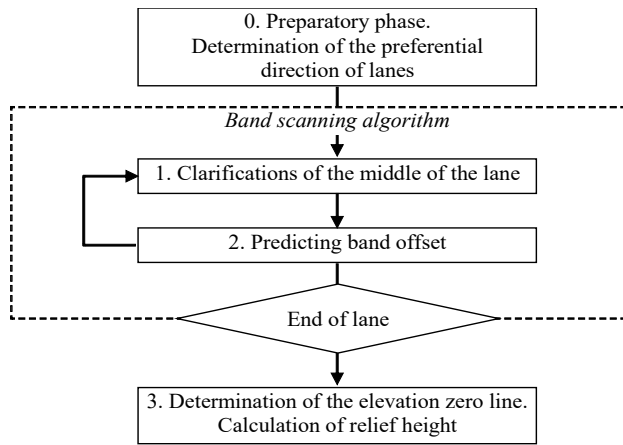


Fig. 6 Block diagram of the algorithm

0. The preparatory stage consists of preliminary photo processing (cropping, brightness and contrast), adjustment of initial parameters of the complex operation and determination of the preferential direction of fringes on the interferogram.

1. Refinement of the interference fringe extremum by quadratic approximation method.

To refine the band extremum  $T$ , we used the  $N$ -point [8] parabola approximation method when the intensity values of several points near the supposed band extremum ( $T$  points in Fig. 7) are used.

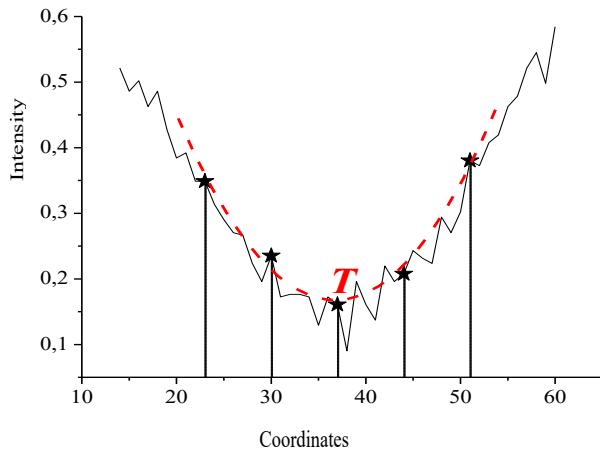


Fig. 7 Intensity distributions along the fringe profile (solid curve) and parabola approximation (dashed line) to refine the fringe  $T$  extremum by five points

2. Predicting the shift of the band extremum at the next point.

After finding the band's extremum, the prediction of the next point's position is built. The prediction allows: 1) track rather abrupt changes in the direction of the fringe course and thereby process fringes of almost any configuration; 2) makes the method robust to single point outliers associated with noise or local defects on the sample surface.

The prediction procedure is shown in Figure 8 and involves the following:

The last  $M$  of the found points  $T_i(x_i, y_i)$ , ( $i=0..M-1$ ), are converted into polar coordinates  $T_i(\rho_i, \phi_i)$ , ( $i=0..M-1$ ), with the centre at the point  $T_0$  by transformation:

$$\begin{cases} \rho_0 = \sqrt{x_0^2 + y_0^2} \\ \rho_i = \sqrt{x_i^2 + y_i^2} - \rho_0 \\ \phi_i = \arctg \frac{x_i}{y_i} \end{cases} \quad (5)$$

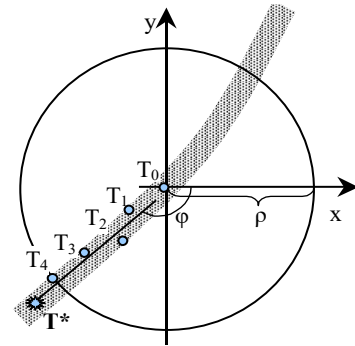


Fig. 8 Illustration of the forecast by  $M=5$  points

Then the prediction of coordinates of the next point  $T^*(\rho^*, \phi^*)$  is produced from the relations:

$$\rho^* = \frac{1}{M-1} \sum_{i=1}^{M-1} \rho_i; \quad \phi^* = \frac{1}{M-1} \sum_{i=1}^{M-1} \phi_i \quad (6)$$

and the inverse transformation of  $T^*$  into Cartesian coordinates  $T^*(x^*, y^*)$  is performed:

$$\begin{cases} x^* = \rho^* \cos \phi^* \\ y^* = \rho^* \sin \phi^* \end{cases} \quad (7)$$

The coordinates  $(x^*, y^*)$  are a prediction of the position of the next strip centre point, which is then refined (see step 1). The described procedure is mathematically equivalent to linear extrapolation of the sequence of points  $T_i$ , ( $i=0..M-1$ ). All fringes in the interference pattern are processed according to the described algorithm.

3. When the fringes are found, it is necessary to determine the zero height level corresponding to the plane from which the surface height change will be calculated (Fig. 9). For each fringe, the line tangent to the interference fringe, obtained by approximating the first  $n$  points of the already refined fringe extremum, is taken as the zero level. This zero level line of the TR is in the form of the equation  $kx + dy + q = 0$ , where  $k$ ,  $d$  and  $q$  are the coefficients of the straight line equation.

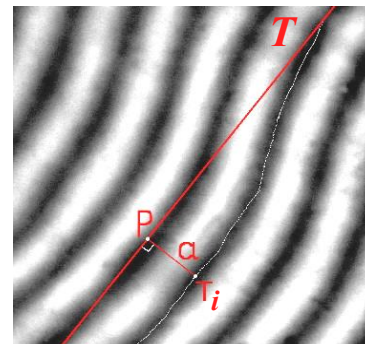


Fig. 9 The zero level line TR and the perpendicular  $a$  drawn to it from the current point of calculation of height  $T_i$  as part of the strip

The height of the relief point of the reconstructed surface on the PT line is taken as the zero level. The heights of the encountered irregularities are counted relative to this zero level.

Calculation of relief (displacement of the point relative to the zero level of the surface) is made by the formula:

$$h_i = \frac{\lambda}{2} \cdot \frac{a_i}{b}, \quad (8)$$

where  $h_i$  is the value of the relative surface height for each point  $i$  of the interference fringe,  $a_i$  is the distance between two points  $P(x_p, y_p)$  and  $T_i(x_T, y_T)$  (Fig. 9),  $b$  is the average value of the interference fringe width.

This principle is used to find the change in surface elevation along each of the interference fringes.

The method of determining the change of height on the surface by the displacement of interference fringes is relative in the sense that the change of height on the surface, i.e. the bending of the interference fringe, is calculated relative to some area on the surface corresponding to the plane where the interference fringes are parallel straight lines. Thus, the method gives the amount of displacement of a point relative to another, so it is necessary to choose fringes that have a section corresponding to the plane, since it is relative to it that the change in height is calculated.

#### Testing of the software complex (numerical experiment)

Testing and validation of the obtained software was carried out by processing of model interference patterns, in which distortions that take place in the real experiment were taken into account.

A numerical experiment was carried out to test the software system. The model of an ideal surface with initially specified step height  $h$  (Fig. 10a) and the corresponding “ideal” interference pattern (Fig. 10b) were constructed.

A set of interference patterns of the surface was constructed with the introduction of various interferences into the resulting pattern: inhomogeneity of illumination and noise of different intensity. The results of processing of these noisy interference patterns were compared

with the “ideal” one. Fig.11 shows the dependence of the error of  $\Delta h$  step height detection on the amplitude of the noise component in per cent of the maximum signal amplitude. The dots show the averaged values of the step height detection error in the interval of noise amplitudes  $0 \div 20\%$ . It follows from the figure that in the given noise amplitude interval the dependence of the averaged error on the noise amplitude is well described by the expression:

$$\Delta h = \Delta h_0 + Ae^{n/t} \quad (9)$$

$$\Delta h_0 = -1.3 \cdot 10^{-4}, \quad A = 0.002, \quad t = 10.8$$

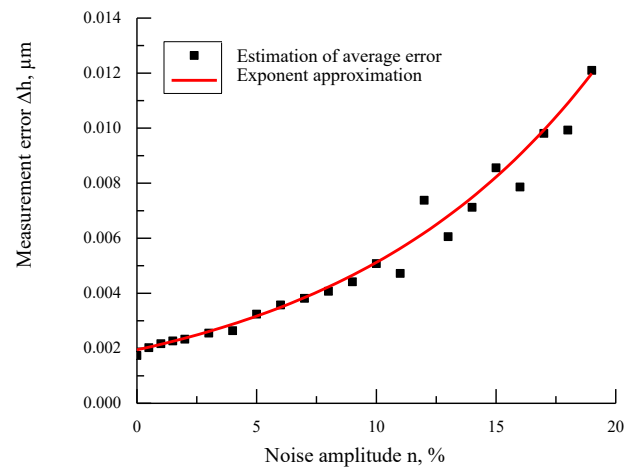


Fig. 11: Graph of averaged values of the error in determining the step (point) height depending on the noise amplitude in the interference pattern (solid line - approximation by an exponent, according to expression (9)).

Studies have shown that a noise amplitude of  $\leq 15\%$  allows the software to correctly process the interference pattern without additional improvements in image quality. Noise amplitude exceeding 20% causes the algorithm to stop tracking fringes. To avoid this, it is necessary to either pre-correct the image with a smoothing filter or increase the number of points used in the prediction. Both of these options, on the one hand, increase robustness to noise, but, on the other hand, do not allow the algorithm to track sharp bends in the fringes.

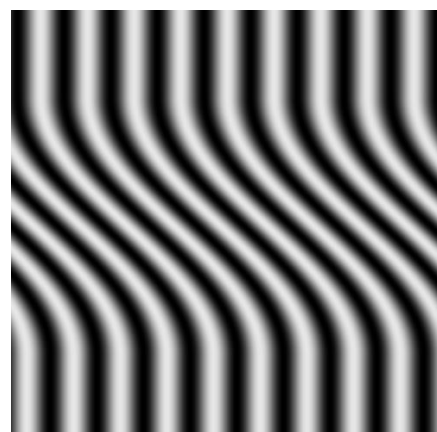
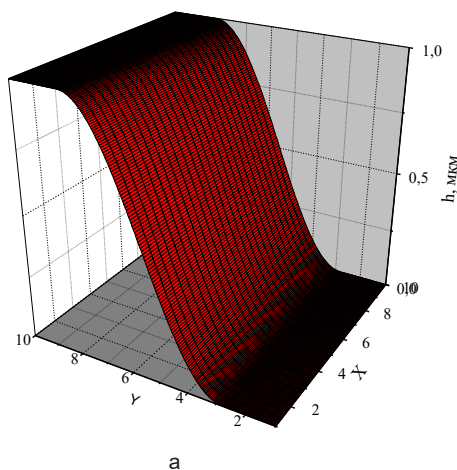


Fig. 10. Model of an ideal surface with a step  $h$  (a) and its corresponding interference pattern (b)

It should be noted that in most of the measurements performed, the accuracy with which the surface is reconstructed (Dh J 0.5%) within 20% of the image noise is sufficient. In case of higher noise levels, additional image preliminary processing is required.

The study of the dependence of the surface profile reconstruction error on the distortion value shows that at distortions close to the real one it is about 0.5%. The mean-square error of profile height determination (repeatability of the results) is  $\sim \lambda/200$ .

### Conclusion

Mathematical and software for automated restoration of surface relief using computer processing of interference pattern photographs have been developed.

A software has been created, which has been tested and approved on the example of surface condition analysis of amorphous metal sample bombarded by deuterium plasma D2. PC has a number of advantages in comparison with known analogues.

In addition to profile reconstruction from the interference pattern image, the software allows to perform its primary processing, for example: display in the form of 3D surfaces with the possibility of rotation and scaling, measurement of distances between points, construction of various sections, smoothing, interpolation, etc. The software can be used to analyse the surface state of an amorphous metal sample. In addition, with the help of the software it is possible to keep an electronic log of the interferometric experiment.

## Моделювання та обробка зображень інтерференційних картин у лінійному інтерферометрі

О. С. Кравченко

Національний технічний університет «Харківський політехнічний інститут», вул. Кирпичова, 2, 61002, Харків, Україна  
[Oleksandr.Kravchenko@cs.khpi.edu](mailto:Oleksandr.Kravchenko@cs.khpi.edu)

### Анотація

Роботу присвячено відновленню профілю рельєфу дзеркальної поверхні за зображенням її інтерференційної картини. Побудовано математичну модель інтерферометра, що дає змогу синтезувати зображення інтерференційної картини за заданим рельєфом поверхні та налаштуваннями мікроінтерферометра. Модель враховує неідеальності оптичного тракту мікроінтерферометра і приймача. Розроблено алгоритм, заснований на спостереженні за інтерференційними смугами, що дає змогу визначити висоту кожної точки зображення відносно нульового рівня, тобто, визначити рельєф поверхні. Створені моделі та алгоритми реалізовано у вигляді програмного комплексу, що дає змогу як моделювати зображення інтерференційних картин, так і відновлювати рельєф поверхні за реальними зображеннями, отриманими за допомогою інтерферометра. Тестування програмного забезпечення здійснювалося за допомогою чисельного експерименту, під час якого використовували параметри рельєфу, схожі з реальними. Створені моделі, методи та програмне забезпечення можуть бути використані як у наукових дослідженнях, так і в заводських лабораторіях, а також для створення навчальних вибірок, для тренування систем машинного зору.

**Ключові слова:** інтерферометрія, інтерференційна картина, синтетичне зображення, комп'ютерний зір, відновлення рельєфу поверхні.

### Reference

1. Belyaeva A., Bardamid A., Davis J., Haasz A., Konovalov V., Kudlenko A., Poon M., Slatin K., Voitseyna V. Hydrogen ion bombardment damage in stainless steel mirrors// *Journal of Nuclear Materials*. 2005. Vol. 345. P. 101-108. Doi: <https://doi.org/10.1016/j.jnucmat.2005.04.066>.
2. Polack F., Thomasset M., Brochet S., Dennetiere D. Surface shape determination with a stitching Michelson interferometer and accuracy evaluation// *Rev. Sci. Instrum*. 2019. Vol. 90, Issue 2. 021708. Doi: <https://doi.org/10.1063/1.5061930>.
3. Salzenstein F., Montgomery P., Montaner D., Boudraa A.-O. Teager-Kaiser Energy and Higher-Order Operators in White-Light Interference Microscopy for Surface Shape Measurement // *EURASIP Journal on Applied Signal Processing*. 2005. Vol. 17. P. 2804–2815. Doi: <https://doi.org/10.1155/ASP.2005.2804>
4. Salzenstein F., Montgomery P., Benatmane A., Boudraa A. 2d discrete high order energy operators for surface profiling using white light interferometry// 7<sup>th</sup> International Symposium on Signal Processing and its Applications, Paris (France), July 1-4, 2003. Vol. 1. P. 601-604. <https://doi.org/10.1109/ISSPA.2003.1224775>
5. Born M., Wolf E., Bhatia A., Clemmow P., Gabor D., Stokes A., Taylor A., Wayman P., Wilcock W. Principles of Optics: Electromagnetic Theory of Propagation, Interference and Diffraction of Light. *Cambridge University Press*, 1999. – 952 p. Doi: <https://doi.org/10.1017/CBO9781139644181>.
6. [https://en.wikipedia.org/wiki/Linnik\\_interferometer](https://en.wikipedia.org/wiki/Linnik_interferometer)
7. Гнеденко Б. Курс теорії ймовірностей. – К.: Видавничо-поліграфічний центр “Київський університет”, 2010. – 464 с.
8. Cohen H. Numerical Approximation Methods. - *Springer New York, NY*, 2011. 485 p. Doi: <https://doi.org/10.1007/978-1-4419-9837-8>.